BPR MCS Bulletin of Pioneering Researches of Medical and Clinical Science

Bulletin of Pioneering Researches of Medical and Clinical Science

Available online: https://bprmcs.com
2024 | Volume 4 | Issue 2 | Page: 124-137

Candidate Protein Biomarkers for Acute Kidney Injury in Patients with Acute Decompensated Heart Failure

Alexander R. Novak[1]*, Sarah J. Bennett[2], Ahmed K. El Sherif[3]

[1]Department of Medical Sciences, Charles University, Prague, Czech Republic.
[2]Department of Clinical Medicine, University of Auckland, Auckland, New Zealand.
[3]Department of Clinical Sciences, Mansoura University, Mansoura, Egypt.

Abstract

Acute kidney injury (AKI) occurs in roughly 25% of patients with acute decompensated heart failure (ADHF), representing a sudden loss of kidney function that correlates with higher long-term mortality. Identifying AKI early in ADHF remains a major clinical challenge, as no protein biomarkers currently offer adequate diagnostic or prognostic reliability for routine use. This study sought to uncover new protein biomarkers for AKI in ADHF by profiling kidney protein changes during disease progression and recovery using a sheep model. Kidney cortices from healthy controls (n = 5), sheep with rapid-pacing-induced ADHF (n = 8), and sheep approximately four weeks post-ADHF recovery (n = 7) were analyzed via SWATH–MS (sequential window acquisition of all theoretical fragment ion spectra–mass spectrometry). Among 790 quantified proteins, 17 were identified as potential markers of kidney injury, one as a candidate for renal recovery, and two as indicators of persistent kidney impairment (fold change 1.2–2.6; adjusted $p < 0.05$). Six of these 20 candidates had prior evidence linking them to AKI, while 14 were novel. Proteins with altered abundance were enriched in inflammatory pathways, including glycoprotein VI (activated during ADHF; adjusted $p < 0.01$) and acute phase response signaling (suppressed during recovery; adjusted $p < 0.01$). These findings may provide new tools for early AKI detection in ADHF and offer insights for improving patient outcomes.

Keywords: Heart failure, Acute decompensated heart failure, Acute kidney injury, Acute renal failure, Biomarker, Proteomics

Corresponding author: Alexander R. Novak
E-mail: alex.novak@outlook.com

How to Cite This Article: Novak AR, Bennett SJ, El Sherif AK. Candidate Protein Biomarkers for Acute Kidney Injury in Patients with Acute Decompensated Heart Failure. Bull Pioneer Res Med Clin Sci. 2024;4(2):124-37. https://doi.org/10.51847/58ShQiHwK7

Introduction

Heart failure affects over 60 million people worldwide [1] and is a leading cause of morbidity and mortality [2]. Among patients experiencing acute decompensation, approximately one in four develops AKI [3, 4], defined as a sudden decline in kidney structure or function. AKI in ADHF nearly doubles one-year mortality risk [5, 6], yet effective therapeutic strategies remain limited [6]. Preventive interventions, such as tailored drug therapy and blood pressure management, are beneficial but no targeted pharmacological treatment exists for AKI [7], largely due to the challenge of detecting early-stage kidney injury. Timely identification of AKI is therefore essential to enable effective intervention and will remain critical as new therapies emerge.

Several renal injury biomarkers have been proposed, including neutrophil gelatinase-associated lipocalin (NGAL), interleukin-18 (IL-18), liver-type fatty acid-binding protein (L-FABP), tissue inhibitor of

metalloproteinases-2 (TIMP-2), insulin-like growth factor-binding protein 7 (IGFBP7), kidney injury molecule-1 (KIM-1), and proenkephalin (PENK) [8–10]. Among these, the urinary combination of TIMP-2 and IGFBP7 (NephroCheck, Astute Medical Inc., USA) is FDA-approved for predicting moderate-to-severe AKI [11]. L-FABP is clinically applied in Japan to monitor AKI in liver failure [9], while NGAL is available in select European regions [12]. However, few studies have assessed these biomarkers specifically in ADHF [13–17], and the AKINESIS trial—the largest to date—found NGAL provided no advantage over plasma creatinine for AKI detection in this context [18].

Despite research into TIMP-2, IGFBP7, and L-FABP for predicting AKI within 1–7 days of ADHF onset [13–17], no biomarker has demonstrated sufficient reliability for routine clinical implementation, with results often inconsistent [19]. Contributing factors include differences in study design, heterogeneous patient populations, varying clinical contexts, and inconsistent definitions of kidney impairment [19]. Overall, the evidence for protein biomarkers in ADHF-related AKI remains insufficient for routine clinical use [19].

This study aimed to identify new protein candidates associated with kidney injury, recovery, and persistent dysfunction in ADHF. Using a sheep model of pacing-induced ADHF, in which kidney function declines immediately and does not fully normalize after ~4 weeks, we employed mass spectrometry to quantify protein changes in kidney tissue. This approach revealed 20 candidate markers, including six previously recognized and 14 novel proteins not previously associated with AKI [20].

Results and Discussion

Physiological results

Physiological and renal data for three groups—healthy control sheep (n = 5; "Baseline"), sheep with pacing-induced ADHF (n = 8; "Heart Failure"), and sheep approximately four weeks post-recovery (n = 7; "Recovery")—are shown in **Figure 1**. This ADHF model has been extensively characterized [20], consistently linking disease induction with subsequent kidney dysfunction. Increases in B-type natriuretic peptide (BNP), plasma renin activity (PRA), and plasma creatinine, along with a marked drop in creatinine clearance, were observed in both paced groups (paired t-tests, $p < 0.05$). Comparisons between the Heart Failure and Recovery groups showed no significant differences in plasma creatinine or creatinine clearance at baseline or at the final pacing day (independent t-tests, $p > 0.14$). After ~4 weeks, BNP and PRA approached baseline levels (paired t-tests, $p = 0.067$ and $p = 0.399$), indicating recovery from HF; however, creatinine clearance remained impaired, showing that renal dysfunction persisted despite resolution of HF (paired t-test, $p = 0.003$).

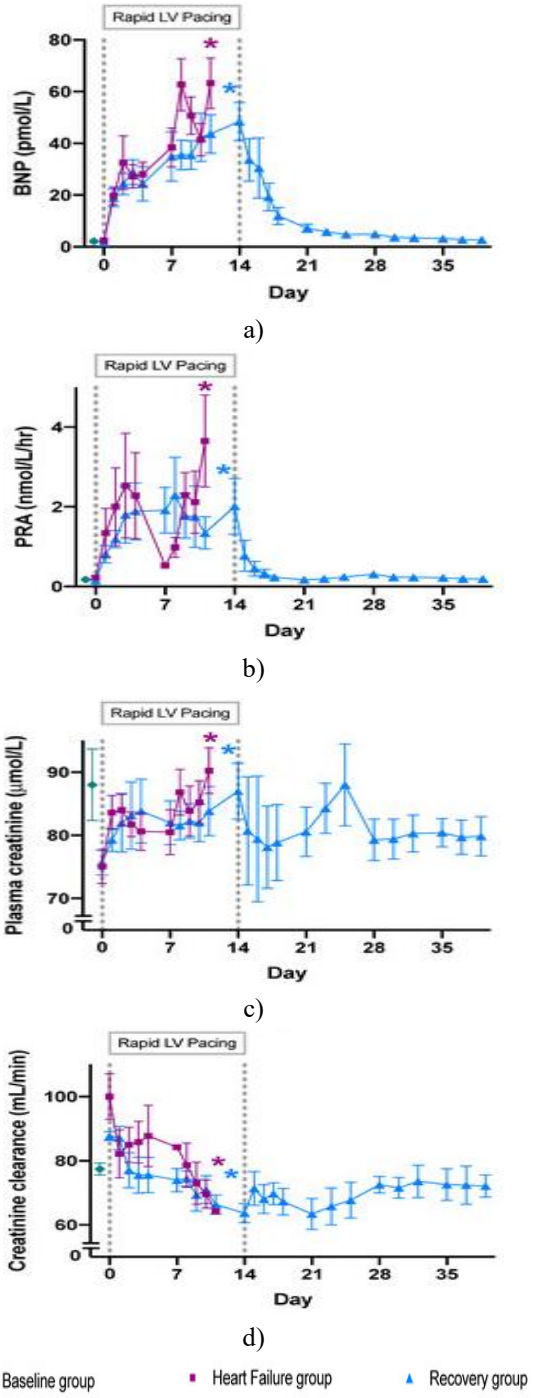

Figure 1. Mean values (± standard error of the mean) for successive physiological measurements in sheep before and during the onset of acute decompensated heart failure (ADHF) induced by pacing, followed by a 25-day recovery period after pacing stopped. A vertical dashed line at day 0 marks the beginning of left ventricular pacing, and another at day 14 indicates when pacing ended. In the Heart Failure group, pacing occurred at 180 beats per minute (bpm) for the first 7 days, then increased to 225 bpm for four days. The

Recovery group received continuous pacing at 220 bpm for fourteen days. The graphs reveal how these physiological parameters changed over time with the start and stop of pacing in each group, with asterisks indicating significant changes relative to day 0 (paired t-tests, $p < 0.05$). Across both paced groups, pacing caused rises in B-type natriuretic peptide (BNP) levels, plasma renin activity (PRA), and plasma creatinine, along with a drop in creatinine clearance. Even though the pacing regimens differed slightly between the Heart Failure and Recovery groups, the resulting kidney damage was similar, as confirmed by no significant group differences in average BNP, plasma creatinine, or creatinine clearance at baseline or the end of pacing (independent t-tests, all $p > 0.14$). BNP= B-type natriuretic peptide; LV= left ventricular; PRA= plasma renin activity.

Identification of Proteins with Altered Abundance

From the 790 proteins consistently measured in the cortical region of sheep kidneys **(Figure 2)**, 52 showed statistically significant changes in levels across the different stages (adjusted $p < 0.05$ for multiple testing; **(Figure 2)**). These proteins were grouped into three patterns based on how their levels shifted during the ADHF timeline: (1) changes occurring only between Baseline and ADHF (but not reversing from ADHF to Recovery), suggesting potential indicators of acute kidney damage; (2) changes from Baseline to ADHF that then reversed from ADHF to Recovery, pointing to proteins involved in renal recovery; and (3) persistent changes from Baseline through to Recovery, indicating possible signs of lasting kidney dysfunction. Specifically, 48 proteins varied between Baseline and ADHF, just 1 varied between ADHF and Recovery, and 7 varied between Baseline and Recovery. Among the 52 proteins, 45 had at least a 1.2-fold change in abundance (**(Table 1)**; this threshold was chosen to focus on the most promising candidates for follow-up).

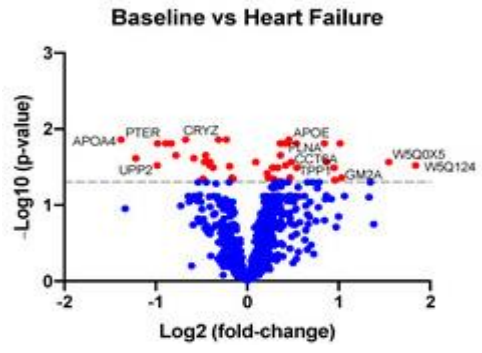

a)

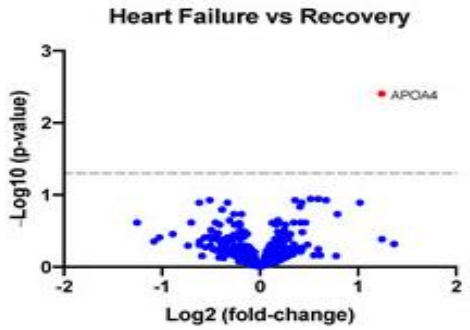

b)

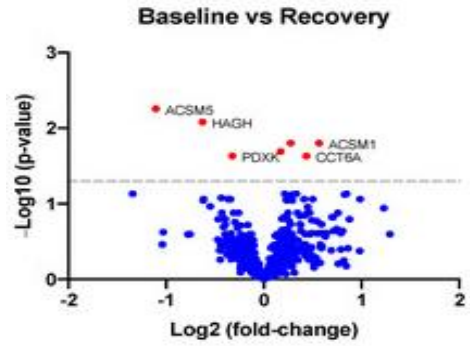

c)

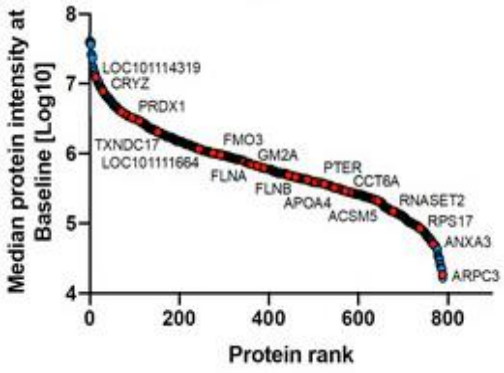

d)

Figure 2. Volcano plots showing the −LOG10 of the Benjamini–Hochberg (BH) adjusted p-value plotted against the LOG2 of the protein fold-change for three comparisons: (a) Baseline versus ADHF, (b) Heart Failure versus Recovery, and (c) Baseline versus Recovery. In these plots, red points denote proteins with a BH-adjusted p-value below 0.05, while blue points represent those with an adjusted p-value of 0.05 or higher. A horizontal dashed line marks the unadjusted p = 0.05 threshold. Panel (d) illustrates that a total of 790 proteins were detected across four orders of magnitude in mass spectrometry intensity. Here, proteins exhibiting significant differential abundance between any time points—defined by a fold-change of at least 1.2 and a BH-adjusted p-value less than 0.05—are highlighted in red; all others (with fold-change below 1.2 and/or adjusted p-value of 0.05 or above) appear in blue.

Table 1. Proteins exhibiting significant differences in abundance across timepoints, with a fold change of at least 1.2 and a Benjamini–Hochberg adjusted p-value below 0.05. B: Baseline; HF: Heart Failure; R: Recovery.

Protein Name	Comparison	Gene	Adjusted p-Value	Fold Change	Enriched in Specific Kidney Cells[2]	Previously Linked to AKI
Upregulated proteins						
Annexin A3	B vs HF	ANXA3	0.01	↑ 1.37		Yes [1] [21]
NTR domain-containing protein	B vs HF	LOC101123672	0.02	↑ 1.79		No
Uncharacterized protein	B vs HF	RNASET2	0.02	↑ 2.02		No
Filamin A	B vs HF	FLNA	0.02	↑ 1.35		No
Apolipoprotein E	B vs HF	APOE	0.02	↑ 1.45	Enriched in proximal tubular cells	Yes [1][22]
Talin 1	B vs HF	TLN1	0.02	↑ 1.30		No
T-complex protein 1 subunit delta	B vs HF	CCT4	0.02	↑ 1.28		No
Ribosomal protein S17	B vs HF	RPS17	0.02	↑ 1.29		No
Chaperonin containing TCP1 subunit 6A	B vs HF	CCT6A	0.03	↑ 1.40		No
	B vs R		0.02	↑ 1.35		
SERPIN domain-containing protein	B vs HF	LOC101115576	0.03	↑ 2.92		No
Actin-related protein 2/3 complex subunit 3	B vs HF	ARPC3	0.03	↑ 1.83		No
Filamin B	B vs HF	FLNB	0.03	↑ 1.34		No
SERPIN domain-containing protein	B vs HF	LOC101119509	0.03	↑ 3.58		No
Integrin beta-1	B vs HF	ITGB1	0.03	↑ 1.21		Yes [1]
Clusterin	B vs HF	LOC101113728	0.03	↑ 1.93		No
Tripeptidyl peptidase 1	B vs HF	TPP1	0.03	↑ 1.46		No
T-complex protein 1 subunit alpha	B vs HF	TCP1	0.03	↑ 1.26		No
Heat shock protein 90 beta family member 1	B vs HF	HSP90B1	0.04	↑ 1.38		Yes [1]
GM2 ganglioside activator	B vs HF	GM2A	0.04	↑ 2.05		Yes [1] [23]
T-complex protein 1 subunit theta	B vs HF	CCT8	0.05	↑ 1.20		No
Thioredoxin domain-containing 17	B vs HF	TXNDC17	0.05	↑ 1.22		No
Vitamin D-binding protein	B vs HF	GC	0.05	↑ 1.94		No
T-complex protein 1 subunit gamma	B vs HF	CCT3	0.05	↑ 1.29		No
Profilin 1	B vs R	PFN1	0.02	↑ 1.21		No
Acyl-CoA synthetase medium-chain family member 1	B vs R	ACSM1	0.02	↑ 1.48		No
Downregulated proteins						
Hydroxyacylglutathione hydrolase	B vs HF	HAGH	0.01	↓ 1.60	Enriched in proximal tubular cells	No
	B vs R		0.01	↓ 1.54		
Apolipoprotein A4	B vs HF	APOA4	0.01	↓ 2.61		Yes [24, 25] [1]

	HF vs R		0.004	↑ 2.36		
Crystallin zeta	B vs HF	CRYZ	0.01	↓ 1.24	Enriched in distal tubular, proximal tubular, and collecting duct cells	No
Phosphotriesterase-related protein	B vs HF	PTER	0.02	↓ 1.97	Enriched in proximal tubular cells	No
Apolipoprotein A2	B vs HF	APOA2	0.02	↓ 1.86		No
Dimethylaniline monooxygenase (N-oxide-forming)	B vs HF	FMO3	0.02	↓ 1.78		No
Glutathione transferase	B vs HF	LOC101111664	0.02	↓ 1.72		No
Solute carrier family 27 member 2	B vs HF	SLC27A2	0.02	↓ 1.37	Enriched in proximal tubular cells	Yes [1]
Aldo-keto reductase domain-containing protein	B vs HF	LOC101109111	0.02	↓ 2.33		No
Sulfurtransferase	B vs HF	TST	0.02	↓ 1.50	Enriched in proximal tubular cells	No
Uncharacterized protein	B vs HF	LOC101114319	0.03	↓ 1.38		No
Solute carrier family 5 member 12	B vs HF	SLC5A12	0.03	↓ 1.36	Enriched in proximal tubular cells	No
Acyl-CoA dehydrogenase domain-containing protein	B vs HF	(partial ID)	0.03	↓ 1.37		No
Dehydrogenase/reductase 1	B vs HF	DHRS1	0.03	↓ 1.33		No
Uridine phosphorylase 2	B vs HF	UPP2	0.03	↓ 1.98	Enriched in distal and proximal tubular cells	No
Uncharacterized protein	B vs HF	(partial ID)	0.03	↓ 1.33		No
Peroxiredoxin 1	B vs HF	PRDX1	0.03	↓ 1.29		Yes [1]
3-Hydroxybutyrate dehydrogenase 1	B vs HF	BDH1	0.05	↓ 1.40		No
Acyl-CoA synthetase medium-chain family member 5	B vs R	ACSM5	0.01	↓ 2.15		No
Pyridoxal kinase	B vs R	PDXK	0.02	↓ 1.25		No

[1] Prior associations were identified by cross-referencing the proteins against a curated list of 884 AKI-related genes derived from the IPA knowledgebase (accessed 16 September 2021) and Harmonizome [26]. [2] Enrichment in specific kidney cell types (proximal tubular, distal tubular, or collecting duct cells) was determined using single-cell expression data from the Human Protein Atlas [27] (accessed 3 November 2021). Arrows denote the direction of change in protein abundance.

Among the 45 proteins that demonstrated a ≥1.2-fold difference between timepoints (adjusted $p < 0.05$), 41 showed changes between Baseline and ADHF, only 1 varied between ADHF and Recovery, and 6 differed from Baseline to Recovery. Only a few proteins overlapped across these intervals, suggesting that the levels of certain proteins may remain consistently altered throughout the progression of ADHF and subsequent recovery.

Pathway activation and inhibition

To examine which kidney molecular pathways are modulated during ADHF onset and recovery, comparative pathway analysis was performed. Of the 790 proteins quantified, 665 could be mapped to genes in the Ingenuity Pathway Analysis (IPA) database and were included in this evaluation. Proteins whose abundance changed across the timepoints were enriched in seven pathways (absolute Z-score > 2 or < −2; adjusted $p < 0.01$); **(Figure 3)**. Two pathways with established links to AKI were notably affected: the glycoprotein VI (GP6) signalling pathway, which is pro-inflammatory and upregulated between Baseline and ADHF [28, 29], and the acute phase response signalling pathway, also pro-inflammatory, which was downregulated from ADHF to Recovery [28, 29]. Other pathways previously associated with AKI that showed suppression between Baseline and ADHF included the anti-inflammatory xenobiotic pregnane X receptor (PXR) pathway [30, 31], the aryl hydrocarbon receptor (AHR) pathway, which has anti-proliferative yet pro-inflammatory effects [32, 33], the anti-inflammatory PPARα/RXRα pathway [34, 35], and the pro-apoptotic, pro-inflammatory protein kinase R (PKR) pathway involved in interferon signaling and antiviral defense [36, 37]. In addition, the coagulation cascade, another pathway implicated in AKI, was activated during the transition from Baseline to ADHF [38, 39].

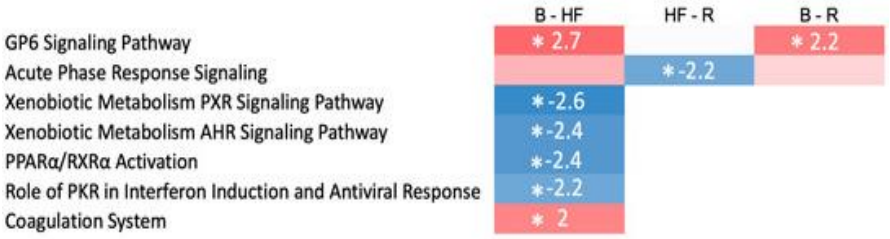

a)

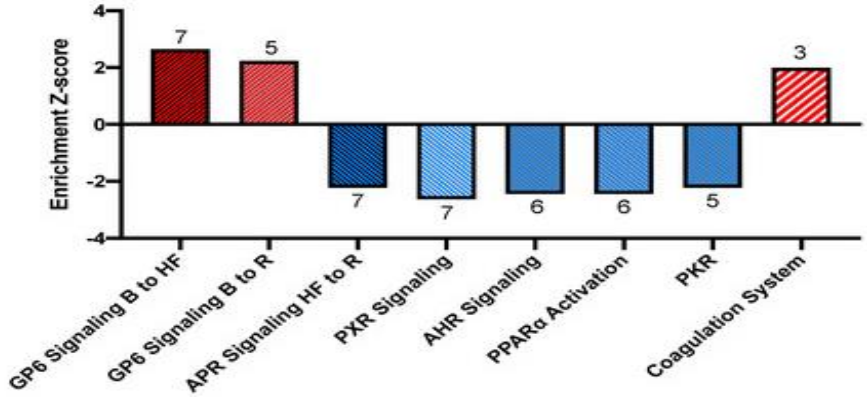

b)

GP6 B to HF	GP6 B to R	APR HF to R	PXR B to HF	AHR B to HF	PPARα B to HF	PKR B to HF	Coagulation B to HF
COL12A1	COL12A1	AHSG	ALDH5A1	ALDH5A1	ACOX1	HSP90AA1	FGA
COL6A2	COL1A2	AMBP	ALDH8A1	ALDH8A1	APOA1	HSP90AB1	FGB
COL6A3	COL6A2	FGA	CAT	GSTM3	GK	HSP90B1	FGG
FGA	COL6A3	FGB	GSTM3	HSP90AA1	HSP90AA1	HSPA5	
FGB	FGA	FGG	HSP90AA1	HSP90AB1	HSP90AB1	HSPA8	
FGG		HPX	HSP90AB1	HSP90B1	HSP90B1		
TLN1		TF	HSP90B1				

c)

Figure 3. (a) A heatmap illustrating the degree of pathway enrichment along with their activation or inhibition status. Each cell shows the corresponding enrichment Z-score, with red reflecting pathway activation and blue reflecting repression; darker shades correspond to stronger Z-scores. Timepoints marked with a star denote an absolute Z-score > 2 or < −2 and an adjusted p-value < 0.01, indicating significantly enriched and modulated pathways. (b) Bar plots of enrichment Z-scores for pathways identified as activated or repressed, with the number of contributing proteins displayed above or below each bar. Red bars indicate activation, while blue bars denote inhibition. (c) Protein lists underlying the annotation of enriched and activated/repressed pathways; proteins involved in multiple pathways are color-coded. Abbreviations: AHR= aryl hydrocarbon receptor signalling pathway; APR= acute phase response signalling pathway; B= Baseline; GP6= glycoprotein 6 signalling pathway; HF= Heart Failure; PKR= protein kinase R pathway; PPARα= peroxisome proliferator-activated receptor alpha; PXR= pregnane X receptor signalling pathway; R= Recovery.

Biomarker discovery

To uncover potential biomarkers for AKI in the context of ADHF, all putative secreted proteins in the dataset were analyzed using the IPA "Biomarker Filter" workflow combined with the Human Protein Atlas secretome [27, 40] (proteinatlas.org). Out of the 45 proteins exhibiting at least a 1.2-fold change ($p < 0.05$), 20 were predicted to be detectable in biofluids such as serum, plasma, or urine and were therefore prioritized as candidate circulating or excreted markers of AKI in ADHF **(Table 2 and Figure 4a)**. Based on their temporal abundance patterns across the ADHF course, these proteins were categorized into 3 groups, resulting in 17 candidates linked to acute kidney injury, 1 associated with recovery, and 2 potentially indicating persistent renal impairment **(Figures 4b–4d)**. To determine prior associations with AKI, these candidates were compared against two large curated datasets: the IPA knowledgebase (https://www.qiagenbioinformatics.com/products/ingenuity-pathway-analysis) (accessed 16 September 2021) and Harmonizome [26]. This screening revealed that 6 proteins had previously documented links to AKI, whereas 14 represented novel biomarker candidates not reported before **(Table 2)**.

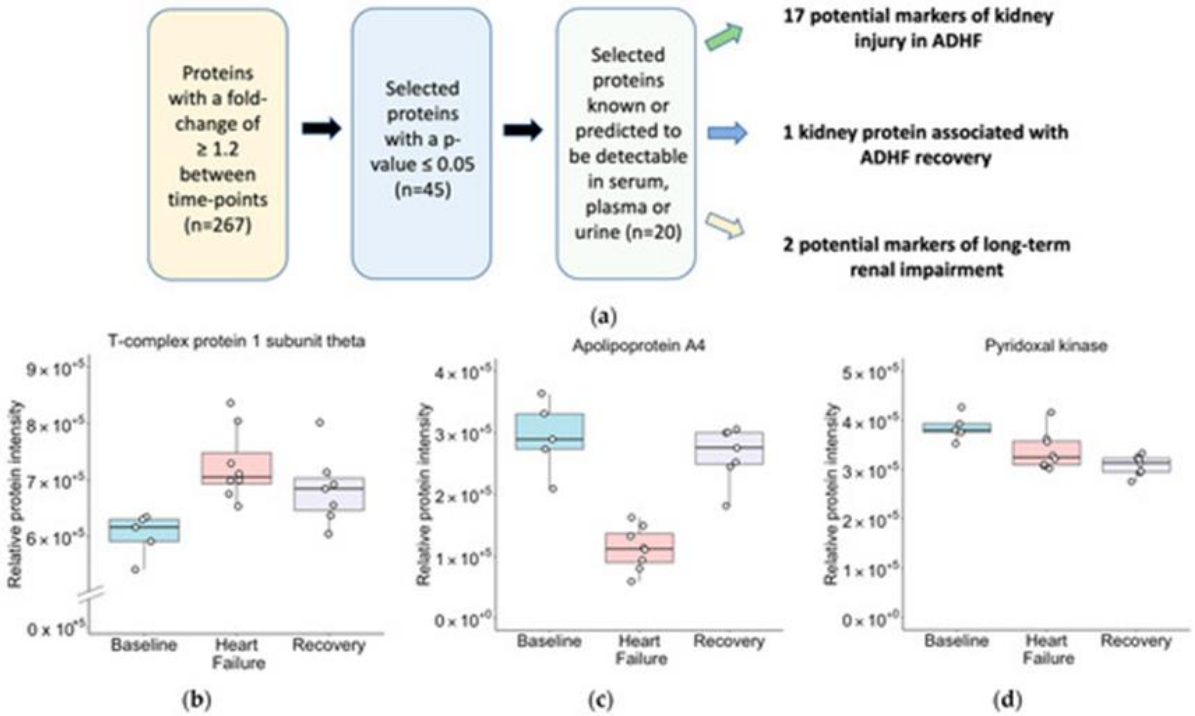

Figure 4. (a) Overview of the process used to identify candidate biomarkers for kidney dysfunction in ADHF. (b–d) Distribution plots of proteins showing significant changes (adjusted $p < 0.05$, fold-change ≥1.2) detectable in plasma, serum, or urine. Panel (b) highlights proteins that differ between Baseline and ADHF but remain unchanged between ADHF and Recovery, suggesting their potential as markers of acute kidney injury during ADHF. Panel (c) depicts proteins that change both from Baseline to ADHF and from ADHF to Recovery, reflecting kidney proteins potentially involved in the recovery phase of ADHF. Panel (d) illustrates proteins with altered abundance between Baseline and Recovery, indicating candidates for long-term renal impairment.

Table 2. Proteins exhibiting a fold-change of at least 1.2 and Benjamini–Hochberg corrected p-values below 0.05, which may be detectable in plasma, serum, or urine.

Category	Protein Name	Time point	Gene	Fold-Change	Previously Linked to AKI	Adjusted p-Value	Category
Potential markers of kidney injury in ADHF							**Potential markers of kidney injury in ADHF**
Upregulated	Filamin A	B-HF	FLNA	↑ 1.35	No	0.02	**Upregulated**
	Apolipoprotein E	B-HF	APOE	↑ 1.45	Yes [22] [1]	0.02	
	Talin 1	B-HF	TLN1	↑ 1.30	No	0.02	
	Filamin B	B-HF	FLNB	↑ 1.34	No	0.03	
	Integrin beta	B-HF	ITGB1	↑ 1.21	Yes	0.03	
	Tripeptidyl peptidase 1	B-HF	TPP1	↑ 1.46	No	0.03	
	T-complex protein 1 subunit alpha	B-HF	TCP1	↑ 1.26	No	0.03	
	Heat shock protein 90 beta family member 1	B-HF	HSP90 B1	↑ 1.38	Yes [1]	0.04	
	GM2 ganglioside activator	B-HF	GM2A	↑ 2.05	Yes [1]	0.04	
	T-complex protein 1 subunit theta	B-HF	CCT8	↑ 1.20	No	0.05	
	Thioredoxin domain containing 17	B-HF	TXND C17	↑ 1.22	No	0.05	
	GC vitamin D binding protein	B-HF	GC	↑ 1.94	No	0.05	

	T-complex protein 1 subunit gamma	B-HF	CCT3	↑ 1.29	No	0.05	
Downregulated	Crystallin zeta	B-HF	CRYZ	↓ 1.24	No	0.01	**Downregulated**
	Apolipoprotein A2	B-HF	APOA 2	↓ 1.86	No	0.02	
	Uridine phosphorylase	B-HF	UPP2	↓ 1.98	No	0.03	
	Peroxiredoxin	B-HF	PRDX 1	↓ 1.29	Yes [1]	0.03	
Kidney proteins associated with ADHF recovery	Apolipoprotein A4	B-HF	APOA 4	↓ 2.61	Yes [24, 25] [1]	0.01	**Kidney proteins associated with ADHF recovery**
		HF-R		↑ 2.36		0.004	
Potential markers of long-term renal impairment	Chaperonin containing TCP1 subunit 6A	B-HF	CCT6 A	↑ 1.40	No	0.03	**Potential markers of long-term renal impairment**
		B-R		↑ 1.35		0.02	
	Pyridoxal kinase	B-R	PDXK	↓ 1.25	No	0.02	

[1] Prior associations were identified by cross-referencing the proteins against a compilation of 884 genes linked to acute kidney injury (AKI), drawn from two extensive databases: the IPA knowledgebase (accessed on 16 September 2021) and Harmonizome [26]

To explore the relationships between the 20 candidate protein markers and established AKI risk indicators, correlation matrices were generated. At Baseline, plasma renin activity correlated positively with heat shock protein 90 beta family 1 and T-complex protein 1 subunit gamma (CCT3), whereas peroxiredoxin showed a positive association with creatinine clearance, and CCT3 was also positively linked to plasma creatinine. During the acute phase of ADHF, GM2 ganglioside activator protein (GM2AP) and crystallin zeta (CRYZ) exhibited positive correlations with plasma creatinine, while pyridoxal kinase correlated with creatinine clearance. Interestingly, CRYZ remained positively associated with plasma creatinine during the recovery period.

This study employed a pacing-induced ovine model of ADHF to uncover candidate protein biomarkers for kidney injury during ADHF, subsequent recovery, and potential long-term renal dysfunction. Using SWATH–MS, 20 proteins were identified whose kidney abundances changed in response to ADHF onset and/or recovery, and which are likely detectable in biofluids, with 14 of these not previously linked to AKI. Among these, 17 proteins were suggested as markers of kidney injury (altered from Baseline to ADHF), 1 as a marker of recovery (altered both from Baseline to ADHF and ADHF to Recovery), and 2 as potential long-term renal impairment indicators (altered between Baseline and 4 weeks post-Recovery). By enabling unbiased, hypothesis-free quantification of moderate-to-high abundance proteins, SWATH–MS provides a comprehensive view of the renal proteome during ADHF, highlighting candidates for diagnostic and prognostic applications in AKI.

The three proteins with the greatest fold-change differences across marker categories were GM2AP (GM2A; candidate marker of kidney injury during ADHF), apolipoprotein A4 (APOA4; marker of recovery), and chaperonin-containing TCP1 subunit 6A (CCT6A; long-term renal impairment marker). APOA4, produced in the small intestine, is a lipid-binding protein involved in lipid metabolism, platelet function, anti-atherosclerotic activity, and glucose regulation [41]. Elevated APOA4 levels have been associated with mild-to-moderate renal impairment and may predict disease progression [24, 25]. GM2AP, a lysosomal glycoprotein cofactor for β-hexosaminidase-mediated GM2 ganglioside degradation [42], has been implicated in tubular injury [43]. Its urinary concentrations rise in AKI due to impaired tubular reabsorption [23], and in combination with CCT7, GM2AP can help predict recovery of renal function following AKI [23].

Unlike APOA4 and GM2AP, CCT6A has not previously been linked to AKI. CCT6A is part of the cytosolic chaperonin-containing T-complex (CCT/TRiC), which facilitates protein folding of key structural proteins like actin and tubulin [44]. The CCT complex consists of eight paralogous subunits (TCP1, CCT2, CCT3, CCT4, CCT5, CCT6A, CCT6B, CCT7, and CCT8) arranged in two stacked rings [45], with each subunit contributing uniquely to cellular function. For instance, CCT6 is essential for actin/tubulin folding and has been linked to fibrotic disease [46], whereas CCT3 influences proliferation and apoptosis [47]. In this study, CCT6A abundance increased 1.4-fold from Baseline to ADHF and remained elevated after 4 weeks of Recovery ($p < 0.05$), suggesting its potential as a marker of persistent renal dysfunction. Additional CCT subunits—CCT3, CCT8, and TCP1—were also among top candidate biomarkers, supporting a potential role for the CCT complex in ADHF-related AKI. This is consistent with prior reports implicating urinary CCT7 (TCP1-eta) as a marker of tubular injury and a

prognostic indicator in AKI when combined with GM2AP [23, 48]; in this study, CCT7 showed a 1.25-fold increase from Baseline to ADHF (adjusted $p = 0.06$).

The proteomic changes observed reflect key inflammatory pathways involved in AKI pathophysiology, which include endothelial injury, tubular cell death, inflammation, and disrupted haemostasis [28, 49]. Notably, the GP6 signalling pathway—a pro-inflammatory cascade—appeared activated during ADHF development, contributing to platelet adhesion and endothelial activation [28], and may persist during recovery, as indicated by enrichment between Baseline and Recovery. Conversely, the acute phase response (APR) signalling pathway, which mediates immune responses to tissue damage [29], was suppressed during ADHF recovery. APR promotes cell death and organ injury via pro-inflammatory mediators, including cytokines, chemokines, reactive species, and enzymes [29]. Proteins within APR that decreased between Baseline and ADHF included hemopexin, alpha-2-HS-glycoprotein, fibrinogen chains (alpha, beta, gamma), and mitochondrial transcription factor A. Fibrinogen contributes to coagulation and is upregulated in AKI [50], whereas hemopexin binds free heme, mitigating oxidative stress and tissue injury [51]. Overall, these changes reflect a transition from inflammatory damage toward renal repair during ADHF progression and recovery, highlighting dynamic regulation of pro-inflammatory pathways in the kidney.

Protein abundance profiles from this study were compared with transcriptomic data previously generated using the same ovine ADHF model [20], revealing that five of the top 20 protein candidates were supported by corresponding gene expression changes. Specifically, the genes encoding CCT6A, filamin A, filamin B, heat shock protein 90 β family member 1 (HSP90B1), and pyridoxal kinase showed ≥1.2-fold alterations (adjusted $p < 0.01$) in kidney tissue during ADHF development and/or recovery. The observed fold-changes at the transcript level were largely consistent in both direction and magnitude with those measured at the protein level; for instance, CCT6A exhibited a 1.4-fold increase in both mRNA and protein between Baseline and ADHF.

To date, studies exploring protein biomarkers for AKI following ADHF have been inconsistent, likely due to the confounding variables inherent in patient-based observational cohorts [19]. A major strength of this study is the use of a controlled ovine model of ADHF [52, 53], which eliminates confounders such as age, sex, ethnicity, comorbidities, and decongestive therapy, simplifying the identification of proteins that respond to kidney injury post-ADHF. Nonetheless, animal models cannot fully recapitulate the complexity of human ADHF, particularly regarding chronic heart failure with episodic decompensation, predisposing factors such as hypertension and arterial disease, and comorbidities commonly present in elderly patients [54]. Furthermore, the sheep in this study did not receive standard ADHF therapies, limiting the direct translatability to the clinical setting [54]. Protein measurements were derived from kidney cortical tissue rather than plasma, and while putatively secreted proteins were prioritized as candidate biomarkers, further studies are needed to confirm whether these renal changes are detectable in circulation or urine.

Several limitations warrant consideration. First, the renal cortex contains diverse cell types—including blood vessels, glomeruli, and tubular epithelium—so protein changes could originate from any of these populations. However, proteins differing in abundance in the cortex remain valid candidates for kidney injury biomarkers, and future studies employing microdissection could clarify cell-specific sources. Second, a sham group was not included due to ethical constraints; some renal changes could reflect anaesthetic or surgical effects. To mitigate this, animals underwent a 14-day recovery period before experimental measurements. Third, the two paced sheep groups experienced slightly different pacing protocols, producing non-identical degrees of renal injury; nevertheless, both groups exhibited consistent, physiologically relevant renal impairment. Finally, translation to clinical practice will require validation of these candidate biomarkers in human samples.

In conclusion, this study has identified multiple candidate protein markers of kidney injury during ADHF, encompassing both proteins previously linked to AKI and novel candidates. Early detection of kidney injury in ADHF could facilitate timely interventions—such as avoiding hypotension or nephrotoxic medications—and inform the design of trials testing renoprotective therapies, ultimately improving patient outcomes [55]. Further research evaluating the presence of these candidates in patient plasma or urine is essential to establish their diagnostic and prognostic value.

Materials and Methods

Experimental animals

All animal procedures were approved by the Animal Ethics Committee of the University of Otago Christchurch (Approval Nos. C23/10 and AUP-19-77). Studies complied with the New Zealand Animal Welfare Act 1999 and Amendment No. 2 (2015), as well as the 8th edition of the National Institutes of Health guidelines.

Baseline control group

Five adult Coopworth ewes (n = 5; “Baseline” group; aged 2–5 years; Lincoln University Farm, Canterbury, New Zealand) were individually housed in metabolic cages for

24 hours to permit full urine collection, with ad libitum access to food and water. After this period, urine was measured for volume and creatinine concentration, and jugular blood samples were obtained for assay of BNP, plasma renin activity (PRA), and creatinine. Euthanasia was then performed using intravenous pentobarbital overdose (150 mg/kg). Renal cortex was harvested immediately, snap-frozen in liquid nitrogen, and stored at −80 °C for later proteomic analysis.

Surgical instrumentation in paced sheep models

Fifteen adult Coopworth ewes (aged 4–6 years, body weight 41–69 kg, obtained from Lincoln University Farm in Canterbury, New Zealand) were subjected to general anesthesia and equipped with devices through a left-sided thoracotomy procedure, following established methods reported in [20, 56]. In essence, a 7-French electrode targeted at the His bundle was affixed to the epicardial surface of the left ventricle to support later pacing interventions, complemented by additional sensors for monitoring hemodynamics and facilitating sample collection. A recovery interval of no less than 14 days was provided post-surgery prior to initiating experimental procedures. Sheep were maintained in individual metabolic cages throughout the study, with constant water availability and a controlled daily ration of pellet feed plus Lucerne chaff (supplying roughly 75 mmol of sodium and 150 mmol of potassium per day).

Experimental design in paced sheep

For the “Heart Failure” cohort (n = 8 sheep), left ventricular pacing was initiated at 180 beats per minute for one week to establish mild, stable heart failure (days 0–7), then escalated to 225 beats per minute for an additional four days to trigger acute decompensated heart failure (ADHF; days 7–11), consistent with prior descriptions in [56]. In the “Recovery” cohort (n = 7 sheep), sustained rapid pacing at 220 beats per minute over 14 days was used to provoke ADHF, after which pacing ceased to allow a 25-day recovery phase [20]. Regular collections of hemodynamic data, blood, and urine were conducted across both timelines [20]. Creatinine clearance (expressed in mL/min) was computed from urinary creatinine concentration multiplied by urine volume, divided by plasma creatinine concentration.

This pacing-induced ADHF paradigm typically manifests as reduced cardiac output, broad activation of neurohormonal systems, avid retention of sodium and fluid, pulmonary congestion with edema, hypotension, increased cardiac filling pressures, and elevated systemic vascular resistance [20, 52]. Critically, renal impairment is a reliable feature: during the ADHF phase, affected sheep show rising plasma creatinine alongside falling creatinine clearance; even after 25 days off pacing, creatinine clearance does not fully normalize [20].

Collection, processing, and preservation of biological samples

Blood destined for hormonal evaluations (atrial natriuretic peptide, brain natriuretic peptide, plasma renin activity) or routine biochemistry (creatinine) was withdrawn into pre-chilled tubes, promptly spun down at 4 °C for 5 minutes, and archived at −80 °C pending assays. Urine volumes were gathered and frozen at −20 °C until required. Upon protocol completion and immediate euthanasia (intravenous pentobarbital 300 at 150 mg/kg), renal cortical tissue was excised, promptly immersed in liquid nitrogen for snap-freezing, and kept at −80 °C in preparation for proteomic mass spectrometry. The harvested cortical specimens included diverse cellular components such as glomeruli, tubular segments, and vascular structures.

Proteomic sample processing

Tissue preparation followed the SPEED (Sample Preparation by Easy Extraction and Digestion) approach outlined by Doellinger *et al*. [57]. Approximately 100 mg of cryopulverized renal cortex was resuspended in trifluoroacetic acid (TFA; Sigma-Aldrich, St. Louis, MO, USA) using a 1:4 volume ratio relative to the sample. Disulfide reduction employed 10 mM Tris(2-carboxyethyl)phosphine (TCEP; Sigma-Aldrich, St. Louis, MO, USA), with simultaneous cysteine alkylation via 40 mM 2-chloroacetamide (CAA; Sigma-Aldrich, St. Louis, MO, USA). Total protein was quantified through turbidity assessment per the original protocol, after which 150 µg was brought to a concentration of 0.75 µg/µL. Enzymatic cleavage used sequencing-grade trypsin (PRV5111, Promega, Fitchburg, WI, USA) at a 25:1 substrate-to-enzyme ratio, incubated overnight at 37 °C for 20 hours.

Mass spectrometry acquisition

Samples received an addition of iRT reference peptides (iRT-Kit, Biognosys, Schlieren, Switzerland) diluted 75-fold from the manufacturer’s stock. SWATH–MS experiments were executed on a TripleTOF 5600+ instrument hyphenated to an Ekspert NanoLC 415 chromatography system (Eksigent, AB Sciex, Dublin, CA, USA), employing a custom 20 cm analytical column packed in-house with 2.6 µm Aeris C18 stationary phase (Phenomenex, Torrance, CA, USA). Chromatographic separation spanned 120 minutes via a binary gradient (mobile phase A: water containing 1% acetonitrile and 0.1% formic acid; mobile phase B: water with 90% acetonitrile and 0.1% formic acid). Reference spectral libraries were built from data-dependent acquisition runs.

SWATH datasets were recorded across a 2-hour separation using dynamic precursor isolation windows. Every sample underwent triplicate analysis, with the median intensity value taken across the three technical replicates for downstream use.

SWATH data processing

Data-dependent acquisition (DDA) files were utilized to create a spectral library using ProteinPilot software (version 4.5, AB Sciex). At a 1.0% false discovery rate, the resulting library encompassed 1777 proteins. SWATH–MS datasets were processed with the SWATH Acquisition™ MicroApp integrated in PeakView software (version 2.2, AB Sciex). To account for potential retention time variations between SWATH–MS acquisitions and the reference library spectra, alignment was performed using ion signals from Biognosys peptides and consistently detected high-abundance endogenous proteins across all samples. The processing parameters in the SWATH Acquisition™ MicroApp were configured as follows: up to 6 peptides per protein, 6 transitions per peptide, a 12-minute extraction window for ion chromatograms, a 1.0% FDR threshold, 75 ppm mass tolerance, and a fixed peptide ranking from the library. Peak areas for transitions, peptides, and proteins were exported to Excel files for subsequent quality assessment and statistical evaluation.

Quality control

Ion intensity values were handled in R [58, 59]. Sample normalization involved scaling each dataset by the ratio of the overall mean ion intensity (based on area under the curve, AUC) across all samples to the AUC of that specific sample. Ions falling below the detection threshold in a sample (defined per ion as the first quartile minus 1.5 times the interquartile range) were removed from that sample. Additionally, ions exhibiting a coefficient of variation exceeding 25% in technical replicates across at least 20% of samples were eliminated from the full dataset. For quantification, the median intensity was assigned to each ion and aggregated to peptide levels, followed by summation of peptide areas to derive protein-level areas [60–62].

Statistical analysis

Statistical procedures were conducted in R [58, 59]. Differential protein abundance across time points (Baseline versus ADHF; ADHF versus Recovery; Baseline versus Recovery) was assessed via three distinct Welch's one-way ANOVA tests implemented in the tableone R package (version 0.13.0) [63]. Resulting p-values underwent Benjamini–Hochberg adjustment to control the false discovery rate, with fold-change values reported accordingly.

Comparison with AKI-related genes

Given the impracticality of validating every differentially abundant protein, priority was given to those showing changes between Baseline and ADHF, ADHF and Recovery, or Baseline and Recovery (with a fold-change of at least 1.2 and an adjusted p-value below 0.05). These selected proteins were cross-referenced against 884 genes linked to acute kidney injury (AKI), sourced from two comprehensive databases: the Ingenuity Pathway Analysis (IPA; Qiagen Inc., https://www.qiagenbioinformatics.com/products/ingenuity-pathway-analysis) knowledge base (accessed 16 September 2021; n = 94) and Harmonizome [26] (n = 814; with 24 genes overlapping between sources).

Identifying enriched and activated/repressed pathways

Canonical pathway enrichment was evaluated using the core and comparison analysis modules in Ingenuity Pathway Analysis software (Qiagen Inc., accessed 16 September 2021). Z-scores were calculated to infer the directional impact of gene expression changes on each pathway, predicting overall activation or inhibition. Z-scores exceeding 2 signified pathway activation, whereas those below −2 indicated repression. A multiple-testing-corrected p-value threshold of less than 0.01 was applied across all IPA evaluations.

Identifying circulating or urinary biomarkers

Candidate biomarkers suitable for detection in circulation or urine were pinpointed through two approaches: (1) the "Biomarker Filter" tool in IPA software, which flags proteins documented in relevant biofluids based on existing literature (mainly [64, 65]), and (2) the Human Protein Atlas secretome dataset (proteinatlas.org), encompassing 2641 proteins predicted to possess a signal peptide without transmembrane domains, including available plasma concentration annotations (via bioinformatics prediction). These compiled potential biomarkers were then cross-compared with the differentially abundant proteins detected in the present investigation.

Acknowledgments: We are grateful to the staff of the University of Otago Christchurch Animal Laboratory for animal care, the staff of our Translational BioDiscovery Laboratory for performing hormone assays, and the Otago Genomics and Bioinformatics Facility (University of Otago-Dunedin, New Zealand) for performing RNA sequencing and assisting with bioinformatics analysis.

Conflict of interest: The Christchurch Heart Institute has agreed in kind support to test proenkephalin (PenKid) as a candidate AKI marker from SphyngmoCor.

Financial support: This research was funded by the National Heart Foundation of New Zealand (grant #1562, #1879, #1693, and #1838), the Health Research Council of New Zealand (grant #14/521, #17/562, #11/170 and #17/562), the Farina Thompson Charitable Trust, the Lotteries Health Research (#R-LHR-2017-49246), the Christchurch Heart Institute Trust, and the University of Otago.

Ethics statement: The study was conducted according to the guidelines of the Declaration of Helsinki, and approved by the Animal Ethics Committee of the University of Otago Christchurch (No. C23/10, approved 1 December 2010; and AUP-19-77, approved 10 June 2019).

References

1. Liu L, Eisen HJ. Epidemiology of heart failure and scope of the problem. Cardiol Clin. 2014;32(1):1–8.
2. Lippi G, Sanchis-Gomar F. Global epidemiology and future trends of heart failure. AME Med J. 2020;5(1):15.
3. McAlister FA, Ezekowitz J, Tonelli M, Armstrong PW. Renal insufficiency and heart failure: prognostic and therapeutic implications from a prospective cohort study. Circulation. 2004;109(8):1004–9.
4. De Silva R, Nikitin NP, Witte KK, Rigby AS, Goode K, Bhandari S, et al. Incidence of renal dysfunction over 6 months in patients with chronic heart failure due to left ventricular systolic dysfunction: contributing factors and relationship to prognosis. Eur Heart J. 2005;27(5):569–81.
5. Gottlieb SS, Abraham W, Butler J, Forman DE, Loh E, Massie BM, et al. The prognostic importance of different definitions of worsening renal function in congestive heart failure. J Card Fail. 2002;8(3):136–41.
6. Richards AM. Biomarkers in acute heart failure—cardiac and kidney. Card Fail Rev. 2015;1(2):107–11.
7. Kashani K, Cheungpasitporn W, Ronco C. Biomarkers of acute kidney injury: the pathway from discovery to clinical adoption. Clin Chem Lab Med. 2017;55(8):1074–89.
8. Endre ZH, Pickering JW, Walker RJ. Clearance and beyond: the complementary roles of GFR measurement and injury biomarkers in acute kidney injury (AKI). Am J Physiol Renal Physiol. 2011;301(4):F697–707.
9. Vanmassenhove J, Vanholder R, Nagler E, Van Biesen W. Urinary and serum biomarkers for the diagnosis of acute kidney injury: an in-depth review of the literature. Nephrol Dial Transplant. 2013;28(2):254–73.
10. Kashani K, Al-Khafaji A, Ardiles T, Artigas A, Bagshaw SM, Bell M, et al. Discovery and validation of cell cycle arrest biomarkers in human acute kidney injury. Crit Care. 2013;17(1):R25.
11. Endre ZH, Pickering JW. Acute kidney injury: cell cycle arrest biomarkers win race for AKI diagnosis. Nat Rev Nephrol. 2014;10(12):683–5.
12. Pickering JW, Endre ZH. Bench to bedside: the next steps for biomarkers in acute kidney injury. Am J Physiol Renal Physiol. 2016;311(4):F717–21.
13. Schanz M, Shi J, Wasser C, Alscher MD, Kimmel M. Urinary [TIMP-2]×[IGFBP7] for risk prediction of acute kidney injury in decompensated heart failure. Clin Cardiol. 2017;40(7):485–91.
14. Hishikari K, Hikita H, Nakamura S, Nakagama S, Mizusawa M, Yamamoto T, et al. Urinary liver-type fatty acid-binding protein level as a predictive biomarker of acute kidney injury in patients with acute decompensated heart failure. Cardiorenal Med. 2017;7(4):267–75.
15. Shirakabe A, Hata N, Kobayashi N, Okazaki H, Matsushita M, Shibata Y, et al. Clinical usefulness of urinary liver fatty acid-binding protein excretion for predicting acute kidney injury during the first 7 days and short-term prognosis in acute heart failure patients without chronic kidney disease. Cardiorenal Med. 2017;7(4):301–15.
16. Shirakabe A, Hata N, Kobayashi N, Okazaki H, Matsushita M, Shibata Y, et al. Worsening renal failure in patients with acute heart failure: the importance of cardiac biomarkers. ESC Heart Fail. 2019;6(3):416–27.
17. Shirakabe A, Hata N, Kobayashi N, Okazaki H, Shinada T, Tomita K, et al. Serum heart-type fatty acid-binding protein level can be used to detect acute kidney injury on admission and predict adverse outcome in patients with acute heart failure. Circ J. 2015;79(1):119–28.
18. Maisel AS, Wettersten N, van Veldhuisen DJ, Mueller C, Filippatos G, Nowak R, et al. Neutrophil gelatinase-associated lipocalin for acute kidney injury during acute heart failure hospitalizations: the AKINESIS study. J Am Coll Cardiol. 2016;68(13):1420–31.
19. Manguba AS Jr, Vela Parada X, Coca SG, Lala A. Synthesizing markers of kidney injury in acute decompensated heart failure: should we even keep looking? Curr Heart Fail Rep. 2019;16(6):257–73.
20. Rademaker MT, Pilbrow AP, Ellmers LJ, Palmer SC, Davidson T, Mbikou P, et al. Acute decompensated heart failure and the kidney: physiological, histological and transcriptomic responses to development and recovery. J Am Heart Assoc. 2021;10(17):e021312.

21. Berger K, Bangen JM, Hammerich L, Liedtke C, Floege J, Smeets B, et al. Origin of regenerating tubular cells after acute kidney injury. Proc Natl Acad Sci U S A. 2014;111(4):1533–8.
22. Isbir SC, Tekeli A, Ergen A, Yilmaz H, Ak K, Civelek A, et al. Genetic polymorphisms contribute to acute kidney injury after coronary artery bypass grafting. Heart Surg Forum. 2007;10(6):E439–44.
23. Blanco-Gozalo V, Casanova AG, Sancho-Martínez SM, Prieto M, Quiros Y, Morales AI, et al. Combined use of GM2AP and TCP1-eta urinary levels predicts recovery from intrinsic acute kidney injury. Sci Rep. 2020;10(1):11599.
24. Boes E, Fliser D, Ritz E, König P, Lhotta K, Mann JF, et al. Apolipoprotein A-IV predicts progression of chronic kidney disease: the mild to moderate kidney disease study. J Am Soc Nephrol. 2006;17(2):528–36.
25. Kronenberg F, Kuen E, Ritz E, König P, Kraatz G, Lhotta K, et al. Apolipoprotein A-IV serum concentrations are elevated in patients with mild and moderate renal failure. J Am Soc Nephrol. 2002;13(2):461–9.
26. Rouillard AD, Gundersen GW, Fernandez NF, Wang Z, Monteiro CD, McDermott MG, et al. The harmonizome: a collection of processed datasets gathered to serve and mine knowledge about genes and proteins. Database (Oxford). 2016;2016(1):baw100.
27. Uhlén M, Fagerberg L, Hallström BM, Lindskog C, Oksvold P, Mardinoglu A, et al. Tissue-based map of the human proteome. Science. 2015;347(6220):1260419.
28. Jansen MPB, Florquin S, Roelofs JJTH. The role of platelets in acute kidney injury. Nat Rev Nephrol. 2018;14(7):457–71.
29. Rabb H, Griffin MD, McKay DB, Swaminathan S, Pickkers P, Rosner MH, et al. Inflammation in AKI: current understanding, key questions, and knowledge gaps. J Am Soc Nephrol. 2016;27(2):371–9.
30. Yu X, Xu M, Meng X, Li S, Liu Q, Bai M, et al. Nuclear receptor PXR targets AKR1B7 to protect mitochondrial metabolism and renal function in AKI. Sci Transl Med. 2020;12(536):eaay7591.
31. Okamura M, Shizu R, Abe T, Kodama S, Hosaka T, Sasaki T, et al. PXR functionally interacts with NF-κB and AP-1 to downregulate inflammation-induced expression of chemokine CXCL2 in mice. Cells. 2020;9(10):2296.
32. Tao S, Guo F, Ren Q, Liu J, Wei T, Li L, et al. Activation of aryl hydrocarbon receptor by 6-formylindolo[3,2-b]carbazole alleviated acute kidney injury by repressing inflammation and apoptosis. J Cell Mol Med. 2021;25(2):1035–47.
33. Larigot L, Juricek L, Dairou J, Coumoul X. AhR signaling pathways and regulatory functions. Biochim Open. 2018;7(1):1–9.
34. Hao Y, Miao J, Liu W, Peng L, Chen Y, Zhong Q. Formononetin protects against cisplatin-induced acute kidney injury through activation of the PPARα/Nrf2/HO-1/NQO1 pathway. Int J Mol Med. 2021;47(2):511–22.
35. Rakhshandehroo M, Knoch B, Müller M, Kersten S. Peroxisome proliferator-activated receptor alpha target genes. PPAR Res. 2010;2010(1):1–20.
36. Zhou J, Zhang F, Lin H, Quan M, Yang Y, Lv Y, et al. The protein kinase R inhibitor C16 alleviates sepsis-induced acute kidney injury through modulation of the NF-κB and NLR family pyrin domain-containing 3 pyroptosis signaling pathways. Med Sci Monit. 2020;26(1):e926254.
37. García MA, Meurs EF, Esteban M. The dsRNA protein kinase PKR: virus and cell control. Biochimie. 2007;89(6–7):799–811.
38. Scrascia G, Rotunno C, Simone S, Montemurno E, Amorese L, De Palo M, et al. Acute kidney injury in high-risk cardiac surgery patients: roles of inflammation and coagulation. J Cardiovasc Med (Hagerstown). 2017;18(5):359–65.
39. Chu LP, Yu YF, Guo LC, Peng JQ, Zhou LF, Wei HY, et al. Predictive value of complement and coagulation indicators in sepsis-related acute kidney injury. Zhonghua Nei Ke Za Zhi. 2020;59(11):854–9.
40. Uhlén M, Karlsson MJ, Hober A, Svensson AS, Scheffel J, Kotol D, et al. The human secretome. Sci Signal. 2019;12(609):eaaz0274.
41. Qu J, Ko CW, Tso P, Bhargava A. Apolipoprotein A-IV: a multifunctional protein involved in protection against atherosclerosis and diabetes. Cells. 2019;8(4):319.
42. Potprommanee L, Ma HT, Shank L, Juan YH, Liao WY, Chen ST, et al. GM2-activator protein: a new biomarker for lung cancer. J Thorac Oncol. 2015;10(1):102–9.
43. Quiros Y, Ferreira L, Sancho-Martínez SM, González-Buitrago JM, López-Novoa JM, López-Hernández FJ. Sub-nephrotoxic doses of gentamicin predispose animals to developing acute kidney injury and to excrete ganglioside M2 activator protein. Kidney Int. 2010;78(10):1006–15.
44. Zhang T, Shi W, Tian K, Kong Y. Chaperonin containing T-complex polypeptide 1 subunit 6A correlates with lymph node metastasis, abnormal carcinoembryonic antigen and poor survival profiles in non-small cell lung carcinoma. World J Surg Oncol. 2020;18(1):1–10.

45. Vallin J, Grantham J. The role of the molecular chaperone CCT in protein folding and mediation of cytoskeleton-associated processes: implications for cancer cell biology. Cell Stress Chaperones. 2019;24(1):17–27.
46. Yi X, Wang Z, Ren J, Zhuang Z, Liu K, Wang K, et al. Overexpression of chaperonin containing T-complex polypeptide subunit zeta 2 (CCT6B) suppresses the functions of active fibroblasts in a rat model of joint contracture. J Orthop Surg Res. 2019;14(1):125.
47. Cui X, Hu ZP, Li Z, Gao PJ, Zhu JY. Overexpression of chaperonin containing TCP1 subunit 3 predicts poor prognosis in hepatocellular carcinoma. World J Gastroenterol. 2015;21(27):8588–604.
48. Sancho-Martínez SM, Sánchez-Juanes F, Blanco-Gozalo V, Fontecha-Barriuso M, Prieto-García L, Fuentes-Calvo I, et al. Urinary TCP1-eta: a cortical damage marker for the pathophysiological diagnosis and prognosis of acute kidney injury. Toxicol Sci. 2019;174(1):3–15.
49. Kinsey GR, Li L, Okusa MD. Inflammation in acute kidney injury. Nephron Exp Nephrol. 2008;109(4):e102–7.
50. Hoffmann D, Bijol V, Krishnamoorthy A, Gonzalez VR, Frendl G, Zhang Q, et al. Fibrinogen excretion in the urine and immunoreactivity in the kidney serves as a translational biomarker for acute kidney injury. Am J Pathol. 2012;181(3):818–28.
51. Zager RA, Johnson ACM, Becker K. Renal cortical hemopexin accumulation in response to acute kidney injury. Am J Physiol Renal Physiol. 2012;303(10):F1460–72.
52. Fitzpatrick MA, Nicholls MG, Espiner EA, Ikram H, Bagshaw P, Yandle TG. Neurohormonal changes during onset and offset of ovine heart failure: role of ANP. Am J Physiol. 1989;256(4 Pt 2):H1052–9.
53. Rademaker MT, Charles CJ, Espiner EA, Frampton CM, Nicholls MG, Richards AM. Natriuretic peptide responses to acute and chronic ventricular pacing in sheep. Am J Physiol Heart Circ Physiol. 1996;270(2):H594–602.
54. Spannbauer A, Traxler-Weidenauer D, Zlabinger K, Gugerell A, Winkler J, Mester-Tonczar J, et al. Large animal models of heart failure with reduced ejection fraction (HFrEF). Front Cardiovasc Med. 2019;6(1):117.
55. Damman K, Testani JM. The kidney in heart failure: an update. Eur Heart J. 2015;36(23):1437–44.
56. Rademaker MT, Ellmers LJ, Charles CJ, Richards AM. Urocortin 2 protects heart and kidney structure and function in an ovine model of acute decompensated heart failure: comparison with dobutamine. Int J Cardiol. 2015;197(1):56–65.
57. Doellinger J, Schneider A, Hoeller M, Lasch P. Sample preparation by easy extraction and digestion (SPEED): a universal, rapid, and detergent-free protocol for proteomics based on acid extraction. Mol Cell Proteomics. 2020;19(1):209–22.
58. R Core Team. R: a language and environment for statistical computing. Vienna: R Foundation for Statistical Computing;2020.
59. RStudio Team. RStudio: integrated development for R. Boston (MA): RStudio Inc.;2018.
60. Ludwig C, Claassen M, Schmidt A, Aebersold R. Estimation of absolute protein quantities of unlabeled samples by selected reaction monitoring mass spectrometry. Mol Cell Proteomics. 2012;11(3):13987.
61. Liu Y, Buil A, Collins B, Gillet L, Blum LC, Cheng L, et al. Quantitative variability of 342 plasma proteins in a human twin population. Mol Syst Biol. 2015;11(1):786.
62. Niu L, Geyer PE, Albrechtsen NJW, Gluud LL, Santos A, Doll S, et al. Plasma proteome profiling discovers novel proteins associated with non-alcoholic fatty liver disease. Mol Syst Biol. 2019;15(3):e8793.
63. Yoshida K, Bartel A. tableone: Create “Table 1” to describe baseline characteristics with or without propensity score weights. R package version 0.13.0; 2021.
64. Anderson NL, Polanski M, Pieper R, Gatlin T, Tirumalai RS, Conrads TP, et al. The human plasma proteome: a nonredundant list developed by combination of four separate sources. Mol Cell Proteomics. 2004;3(4):311–26.
65. Omenn GS, States DJ, Adamski M, Blackwell TW, Menon R, Hermjakob H, et al. Overview of the HUPO plasma proteome project: results from the pilot phase. Proteomics. 2005;5(13):3226–45.